Available online at www.sciencedirect.com

ScienceDirect

Mendeleev Commun., 2024, **34**, 174–177

Mendeleev Communications

Synthesis, optical and electrochemical properties of regioisomeric methanofullerene derivatives of C_s-$C_{70}(CF_3)_8$

Sofia V. Gracheva, Nadezhda B. Tamm, Maria P. Kosaya, Alexey V. Rybalchenko, Nikita M. Belov, Natalia S. Lukonina* and Alexey A. Goryunkov

Department of Chemistry, M. V. Lomonosov Moscow State University, 119991 Moscow, Russian Federation.
E-mail: nsovchinnikova@gmail.com

DOI: 10.1016/j.mencom.2024.02.005

The Bamford–Stevens reaction with C_s-$C_{70}(CF_3)_8$ provides four regioisomeric cyclopropanated and at least one bis-cyclopropanated polyfunctional derivatives $C_{70}(CF_3)_8DPM_n$, $n = 1, 2$ [DPM = $C(p\text{-}MeOC_6H_4)_2$]. A strong influence of the addition patterns on fluorescence and electrochemical properties is demonstrated for three spectrally identified monoadducts $C_{70}(CF_3)_8DPM$.

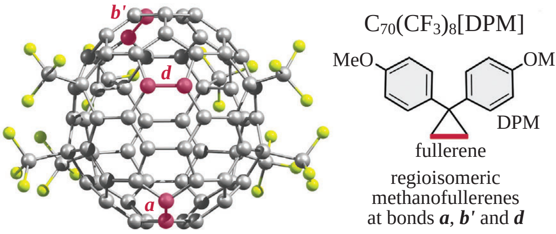

Keywords: methanofullerene, trifluoromethylated fullerene, addition pattern, fluorescence, cyclic voltammetry.

Fullerenes and their derivatives are well-known organic *n*-type semiconducting materials, which are used for fabrication of numerous organic optoelectronic devices, *e.g.* polymer and perovskite solar cells, light-emitting diodes, field-effect transistors, *etc.*[1–6] Tuning of the electronic and optical properties of the fullerene derivatives is provided by variability of addition patterns tailoring a series of πe-conjugated systems with different size and connectivity at fullerene cage. Isomeric diversity of fullerene polyfunctional derivatives provides a representative set of compounds to study correlation between the addition patterns and the electronic properties of the compounds. A wide variation of the electron-withdrawing abilities and optical gaps was shown for large sets of trifluoromethylated fullerenes $C_{60}(CF_3)_{2n}$ ($2n = 2$–12)[7,8] and $C_{70}(CF_3)_{2m}$ ($2m = 2$–20).[7,9] As was reported in the pioneer work by A. Popov *et al.*,[10] isomeric trifluoromethylated fullerenes $C_{70}(CF_3)_8$ and $C_{70}(CF_3)_{10}$ reveal the dramatic variability of fluorescence spectra and quantum yields. High variability of fluorescence properties regarding the addition patterns was reported for polyfunctional mono-, bis- and tris-cyclopropane derivatives of C_s-$C_{70}(OMe)_8$ by L. Gan *et al.*[11] Strong effect of a πe-conjugated system connectivity on the electrochemical and fluorescent properties of structurally related C_s-$C_{70}(CF_3)_8[X]$ compounds with near-equatorial addition of bivalent addend X, where X is $>CF_2$ and $>C(p\text{-}MeOC_6H_4)_2$ (aka DPM), had been studied in our previous works.[12–14]

Here we report the structure, electronic and electrochemical properties of two cyclopropanated adducts of DPM moiety to C_s-$C_{70}(CF_3)_8$ at the bonds ***a*** and ***b′*** in comparison with the major adduct at the near-equatorial bond ***d***,[13,14] which have been obtained by the reaction of C_s-$C_{70}(CF_3)_8$ (Figure 1) with 4,4′-dimethoxybenzophenone tosylhydrazone in the presence of a base.

Two alternative approaches to cyclopropanation of fullerenes are widely used. The nucleophilic cyclopropanation of fullerenes *via* addition of stabilized α-halocarboanion followed by intramolecular nucleophilic substitution closing of cyclopropane ring at [6,6]-double bond of fullerene was developed by C. Bingel and further modified by A. Hirsch (aka the Bingel and the Bingel–Hirsch reactions[15–17]). A different approach to preparation of fulleroids and methanofullerenes was proposed by Hummelen and Wudl,[18] who first used the Bamford–Stevens reaction for fullerene derivatization. The base-induced decomposition of tosylhydrazones of ketones produces reactive diazoalkanes which react with fullerene substrate by two alternative pathways,[19,20] *viz.* (i) a 1,3-dipolar addition of diazoalkane at [6,6]-double bond of fullerene giving a thermally labile pyrazoline intermediate which undergoes kinetically controlled N_2-extrusion resulting in thermodynamic unstable fulleroid; (ii) thermal-induced decomposition of diazoalkane giving carbene intermediate which is rapidly trapped *via* [2 + 1] cycloaddition at [6,6]-double bond yielding the thermodynamically stable methanofullerene. In addition, prolonged refluxing of fulleroid results in its isomerization into the most thermodynamically stable methanofullerene.[21]

Both the Bingel–Hirsch and Bamford–Stevens reactions have been successfully employed for trifluoromethylfullerenes.[22,23] Bulky $CBr(COOR)_2^-$ carbanion attacks the pole carbon atoms of C_s-$C_{70}(CF_3)_8$ followed by cyclopropanation at the bonds ***a*** and ***b′***, while [2 + 1] cycloaddition of more compact **:**$C(p\text{-}MeOC_6H_4)_2$

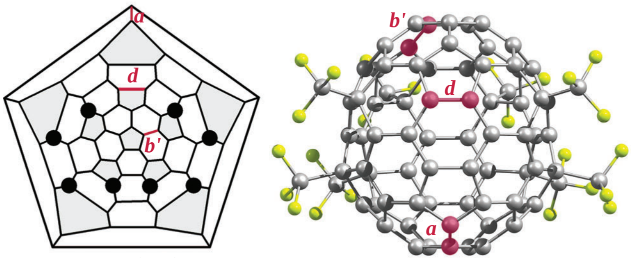

Figure 1 The Schlegel diagram (black circles denote position of CF_3 groups) and the projection of C_s-$C_{70}(CF_3)_8$ with highlighted most reactive bonds ***d***, ***a***, and ***b′***.

carbene occurs at the most reactive near-equatorial bond ***d*** which is sterically hindered by two terminal CF_3 groups (see Figure 1). It is worth noting that the bond ***d*** has low reactivity in pristine C_{70},[24,25] but it is activated by the near-equatorial addend pattern of eight groups in C_s-$C_{70}X_8$ fullerenes. The various tiny reactive species like H, Cl, O, CH_2, or CF_2 rapidly reacts exclusively at the bond ***d*** in C_s-$C_{70}(OMe)_8$[11] and C_s-$C_{70}(CF_3)_8$.[12,13,23,26,27] Thus, near-equatorial arrangement pattern in C_s-$C_{70}X_8$ has activating and orienting effects on the addition at the pole or near-equatorial bonds depending on the size of reactive species.

One can suppose that addition of intermediate size **:**$C(p\text{-}MeOC_6H_4)_2$ carbene would provide a larger isomeric diversity during C_s-$C_{70}(CF_3)_8$ derivatization in the Bamford–Stevens reaction. To verify this assumption, we performed the reaction of C_s-$C_{70}(CF_3)_8$ with 4,4′-dimethoxybenzophenone tosylhydrazone in the presence of K_2CO_3 and pyridine as bases under refluxing in *ortho*-dichlorobenzene (see Online Supplementary Materials for the experimental details). Indeed, HPLC trace of the reaction mixture (Figure 2) revealed formation of several products beside the early eluted major monoadduct at the bond ***d*** (**1**) which was recently studied in detail.[13,14]

The individual compounds were isolated and purified by semi-preparative HPLC and their molecular compositions were determined using MALDI mass spectrometry (Table 1 and Figure S1). Four isomeric monoadducts $C_{70}(CF_3)_8$DPM (**1**, **2**, **4**, **5**) as well as one bisadduct $C_{70}(CF_3)_8DPM_2$ (**3**) were isolated in the appreciable yields.

Unfortunately, none of the fractions with previously unknown compounds **2**–**5** gave crystalline material suitable for the single crystal X-ray diffraction analysis. Therefore, the structures of novel compounds were ascertained by NMR and UV/VIS spectroscopy. Scanty information can be obtained from the chemical shift value of quartet signal of terminal CF_3 group (which has only one neighboring CF_3) and its spin–spin coupling constant. UV/VIS spectra of the fullerene compounds being fingerprinting for given addition patterns (due to the presence of the conjugated πe-system with given size and connectivity) provide essential information for structural elucidation. Taking into accounts the previously reported spectral data for related well-characterized derivatives of C_s-$C_{70}(CF_3)_8$, we have reliably identified two monoadducts II (**2**) and IV (**5**).

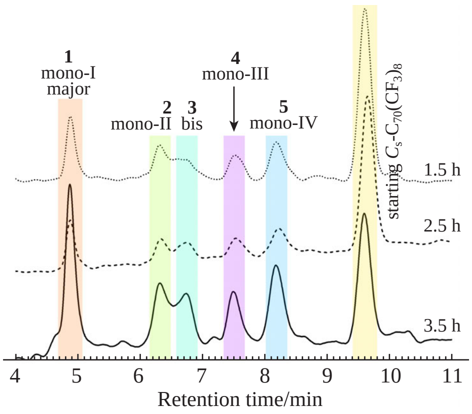

Figure 2 The HPLC monitoring of reaction mixture (Cosmosil Buckyprep 4.6 mm i.d. × 25 cm, toluene : hexane = 1 : 1 v/v, 1 ml min^{-1}, 290 nm).

According to ^{19}F and ^{1}H NMR data (Figure S2), monoadduct II (**2**) is C_s-symmetrical compound with equivalent OMe groups of DPM moiety evidencing cyclopropanation at the C–C double bond in mirror plain of the molecule. There are only two C–C double bonds laying in the mirror plain of the molecule and both situated at the poles of the molecule. Among them the lowest relative formation energy corresponds to the addition at the bond ***a*** (20.7 kJ mol^{-1} at PBE/TZ2p DFT level,[28,29] it is the second by relative energy formation isomer of $C_{70}(CF_3)$DPM), while the adduct at the another C–C double bond is less thermodynamically preferable (33.9 kJ mol^{-1}).[13] The ^{19}F NMR spectrum of **2** consist of one quartet and three multiplet signals of equal integral intensity. The quartet resonance was attributed to pair of equivalent terminal CF_3 groups, whose δ_F value and J_{FF} constant are similar to those for C_s-$C_{70}(CF_3)_8$ (see Table 1). The ^{1}H NMR spectrum contains one singlet at 3.78 ppm of two equal OMe groups and appropriate set of signals for aromatic protons. Finally, the UV/VIS spectrum is analogous to that of the C_s-$C_{70}(CF_3)_8[C(CO_2Et)_2]$ cycloadduct at the bond ***a*** evidencing the same addition pattern in compound **2** (see Figure S4). Likewise, the quartet of two equivalent terminal CF_3 groups for C_s-$C_{70}(CF_3)_8[C(CO_2Et)_2]$ adduct at the bond ***a*** appears at –66.04 ppm with J_{FF} value of 16.1 Hz.[23]

The ^{19}F NMR spectrum of monoadduct IV (**5**) evidences its trivial symmetry (Figure S3). It contains one unresolved multiplet corresponding to two CF_3 groups in very similar environment, two resolved quartet and four multiplet resonances of the rest six CF_3 groups. The two quartets of terminal CF_3 groups are observed at –64.61 and –66.78 ppm with coupling constant values of 13.9 and 16.0 Hz, respectively. The set of ^{1}H NMR signals relates to the cyclopropanated derivative $C_{70}(CF_3)_8$DPM with trivial symmetry as well. Despite a lot of isomeric monoadducts corresponds to the NMR pattern of compound **2**, it has been identified as an adduct at the bond ***b′*** due to coincidence of its UV/VIS spectrum with those for the previously structurally characterized C_s-$C_{70}(CF_3)_8[C(CO_2Et)_2]$ adduct at the bond ***b′*** (Figure S4).[23] The diagnostic quartets in the ^{19}F NMR spectrum of the Bingel adduct at the bond ***b′*** appear at –66.35 (16.1 Hz) and –66.64 ppm (15.5 Hz).[23] Small differences of J_{FF} values for quartets of terminal CF_3 group neighboring to the cyclopropane moiety arise from differing sterical hindrance of carboethoxy and *p*-methoxyphenyl groups.

Both the monoadducts **2** and **5** have been predicted among the most energetically favorable isomers at the second and third places by relative energy after the most stable monoadduct **1** according to the DFT calculations (20.7 and 24.8 kJ mol^{-1}, respectively, at PBE/TZ2p).[13] Next by energy isomeric cycloadducts corresponding to the addition at the pole

Table 1 Identification of the isolated products.

Compound	Site[a]	t_R/min[b]	Yield (%)[c]	Composition[d]	$-\delta_F$/ppm[e]	δ_H/ppm[e]	Reference
mono-I (**1**)	***d***	4.9	26	$C_{70}(CF_3)_8$DPM	66.57 ($2CF_3$, 15.6)	3.82 (3H), 3.72 (3H)	13, 14
mono-II (**2**)	***a***	6.3	12	$C_{70}(CF_3)_8$DPM	66.13 ($2CF_3$, 16.5)	3.78 (6H)	this work
bis-I (**3**)	N.I.	6.7	11	$C_{70}(CF_3)_8DPM_2$	–	–	this work
mono-III (**4**)	N.I.	7.5	10	$C_{70}(CF_3)_8$DPM	–	–	this work
mono-IV (**5**)	***b′***	8.2	16	$C_{70}(CF_3)_8$DPM	64.61 (CF_3, 13.9), 66.78 (CF_3, 16.0)	3.82 (3H), 3.74 (3H)	this work
C_s-$C_{70}(CF_3)_8$	–	9.6	22	$C_{70}(CF_3)_8$	65.74($2CF_3$, 16.1)	–	13

[a] Attachment site at the respective bonds as denoted in Figure 1 (N.I. – not identified). [b] HPLC retention time, Cosmosil Buckyprep 4.6 mm i.d. × 25 cm, toluene : hexane = 1 : 1 v/v, 1 ml min^{-1}. [c] According to HPLC trace integration. [d] According to MALDI MS data. [e] NMR $-\delta_F$ and δ_H shifts of the diagnostic terminal CF_3 and OMe groups (J_{FF} coupling constants are given in Hz).

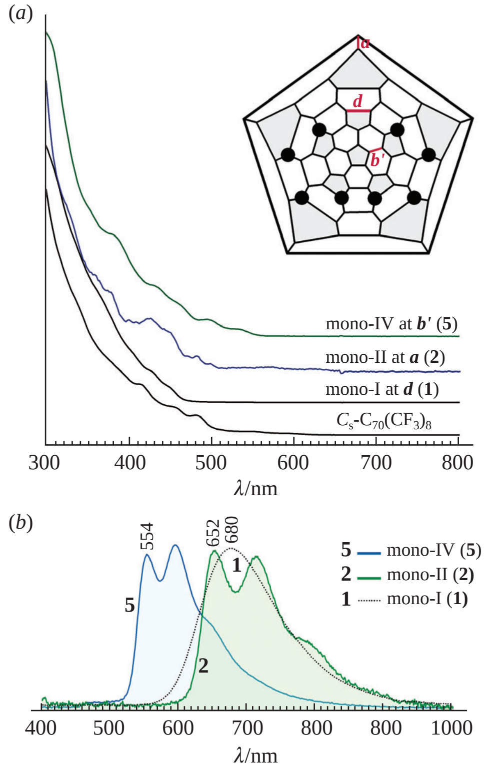

Figure 3 (*a*) The electronic absorption (the Schlegel diagram of C_s-$C_{70}(CF_3)_8$ with marked cyclopropanation sites ***a***, ***d***, and ***b′*** is shown in inset) and (*b*) fluorescence spectra of monoadducts **2** and **5** in comparison with the major one **1** (cyclohexane, excitation at 355 nm).

Table 2 The optical properties of C_s-$C_{70}(CF_3)_8$ and $C_{70}(CF_3)_8$DPM isomers.

Compound	E_g/eV	λ_{abs}/nm	λ_{em}/nm	The Stokes shift/cm^{-1}	Φ_f	Reference
mono-I (**1**)	2.6	448	680	7616	0.051	13, 14
mono-II (**2**)	1.9	615	652	923	0.005	this work
mono-IV (**5**)	2.2	534	554	676	0.009	this work
C_s-$C_{70}(CF_3)_8$	2.0	595	613	494	0.0012	10

[6,6]-bonds have slightly larger formation energies (28–29 kJ mol^{-1}) and can be expected among unidentified product **4** of the reaction. Structurally unidentified bisadduct **3** can be the product of cyclopropanation at two different sites from the bonds ***a***, ***b′***, and ***d***.

The electronic absorption, fluorescence spectra and optical properties of monoadducts **2** and **5** along with previously characterized monoadduct **1**[14] and parent C_s-$C_{70}(CF_3)_8$[10] are presented in Figure 3 and Table 2. Cyclopropanation at the bond ***b′*** (compound **5**) provides vibrationally resolved emission peaked at 554 nm, which is significantly blue-shifted in comparison with parent C_s-$C_{70}(CF_3)_8$. However, the Stokes shift is still rather low due to strong rigidity of the molecule. Functionalization of the bond ***a*** at the opposite pole of the molecule (compound **2**) reveals weak perturbation of the π-system compared to C_s-$C_{70}(CF_3)_8$ and structurally flexible monoadduct at the bond ***d***, in which initial 62πe-system remains at the excitation.

Finally, the influence of cyclopropanation of C_s-$C_{70}(CF_3)_8$ on electronic properties was studied by means of cyclic voltammetry (CVA) for polyfunctionalized derivatives **2** and **5** and the results were compared with the previously reported data for parent C_s-$C_{70}(CF_3)_8$[30] and major monoadduct I (**1**)[13] (Figure 4 and Table 3). All compounds exhibit at least two reversible one-electron reduction processes, which indicates the stability of the compounds in mono- and dianionic states with respect to the loss of addends. The third reductions are reversible for C_s-$C_{70}(CF_3)_8$ and its adducts **1** and **2** whereas formation of trianionic species of **5** is accompanied by appearing the reoxidation peak at *ca*. –2.0 V which can be assigned to the C_s-$C_{70}(CF_3)_8^{3-/2-}$ couple.

Among the obtained derivatives, compound **1** shows the lowest electron-withdrawing ability, in which the electrochemically estimated LUMO energy is raised for 0.34 V with respect to the LUMO of C_s-$C_{70}(CF_3)_8$.[13] This is due to dividing 62πe-system of C_s-$C_{70}(CF_3)_8$ *via* cyclopropanation of the near-equatorial [5,6]-double bond ***d*** to yield [5,6]-closed adduct **1**

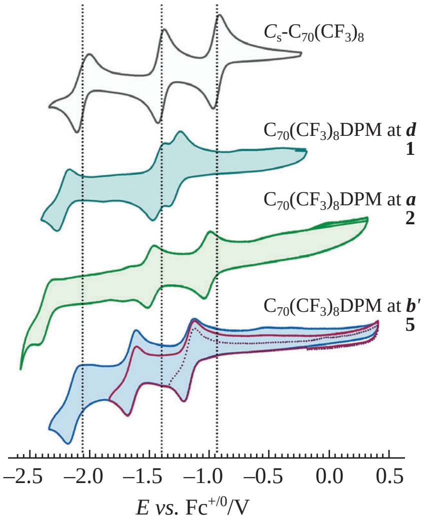

Figure 4 The CVA curves for C_s-$C_{70}(CF_3)_8$ and $C_{70}(CF_3)_8$DPM isomers **1**, **2** and **5** (Pt, *o*DCB, 0.2 M Bu_4NBF_4, 100 mV s^{-1}).

Table 3 The formal reduction and oxidation potentials of C_s-$C_{70}(CF_3)_8$ and its cycloadducts under study.[a]

Compound	*E* vs. Fc$^{+/0}$/V					E_1 *vs.* C_s-$8^{0/-}$/V	Electrochemical MO[b]/eV		Reference
	Ox2	Ox1	0/–	–/2–	2–/3–		LUMO	HOMO	
C_s-$C_{70}(CF_3)_8$	[1.50]	–	–0.95	–1.41	–2.08	0	–4.22 [–3.95] {–4.56}	–6.52 [–6.99]	30
mono-I (**1**)	N.A.[c]	N.A.	–1.29	–1.43	–2.22	–0.34	–3.88 {–3.96}	N.A. {–5.56}	13
mono-II (**2**)	[1.48]	[1.32]	–1.02	–1.49	–2.37	–0.07	–4.16 {–4.3}	–6.33	this work
mono-IV (**5**)	[1.49]	[1.34]	–1.17	–1.65	[–2.13]	–0.22	–3.98 {–3.90}	–6.35	this work

[a] Pt, *o*DCB, 0.2 M Bu_4NBF_4, *vs.* Fc$^{+/0}$, 100 mV s^{-1}, 25–30 °C. The potential values of the irreversible processes are given in the square brackets. C_s-$8^{0/-}$ denotes C_s-$C_{70}(CF_3)_8^{0/-}$ couple. [b] The electrochemical levels of the boundary molecular orbitales (MO) in the Fermi scale were estimated using the onsets of the first reduction and oxidation potentials according to equation $E_{MO} = -(E_{onset} + 5.1)$ eV.[31] The energies of the boundary MOs were calculated at the DFT[32–35] levels using PBE0/def2-SVP//PBE/TZ2P and PBE/TZ2P (values in square and curly brackets). [c] N.A. – not available.

with isolated 32- and 28πe-subunits.[13] Cyclopropanation at sites ***a*** and ***b′*** shrinkages πe-conjugated systems, which decreases electron-withdrawing abilities of the derivatives raising the electrochemically estimated LUMO energies for 0.07 and 0.22 eV for **2** and **5**, respectively, against that for parent C_s-$C_{70}(CF_3)_8$. Indeed, DFT-calculated LUMO energies for compound under study fairly fit with the electrochemically estimated LUMO energies (see Figure S7).

The separation of *ca.* 0.47–0.48 V between the first and the second reductions for compounds **2** and **5** is similar to that for C_s-$C_{70}(CF_3)_8$ thus indicating preservation of the size and connectivity of π-electron conjugated systems of fullerene framework during negative charging of the compounds. On the contrary, the reduction of isomer **1** is accompanied by the dissociation of C–C bond, which transforms [5,6]-closed configuration of methanofullerene into [5,6]-open configuration retaining 62πe-conjugated system with enhanced electron-withdrawing ability and respective narrowing the gap between the first and second reduction to 0.13 V.[13]

Anodic oxidation of compounds **2** and **5** reveals two irreversible oxidations at the potentials of *ca.* +1.3 and +1.5 V *vs.* $Fc^{+/0}$ for both compounds (see Table 1 and Figures S5, S6). The parent C_s-$C_{70}(CF_3)_8$ exhibits the irreversible oxidation at *ca.* +1.5 V *vs.* $Fc^{+/0}$ assigned to oxidation of fullerene cage.[30] Therefore, we attributed the first and the second oxidations of DPM-derivatives to oxidation of *para*-methoxyphenyl moiety and fullerene cage.

Thus, the Bamford–Stevens reaction with C_s-$C_{70}(CF_3)_8$ provides cyclopropanation at the near-equatorial [5,6]-double bond and at two [6,6]-double bonds at the opposite pole of the molecule. This pathway leads to a larger isomeric diversity of the cyclopropanated polyfunctionalized fullerene derivatives in contrast to the Bingel–Hirsch reaction. The optic properties and electron-withdrawing abilities of the $C_{70}(CF_3)_8$DPM isomers are strongly dependent on the cyclopropanation site. Addition at the opposite sites of the fullerene cage leads to isomers with significantly differing LUMO level energies (0.15 eV) and LUMO–HOMO gaps (0.3 eV), whereas the larger variability was found for the near-equatorial adduct (0.3 and 0.4 eV, respectively). It indicates that the isomeric polyfunctional derivatives will demonstrate significantly different chemical behavior as well as optical and electronic properties.

N.S.L., M.P.K. and S.V.G. gratefully acknowledge financial support of this work by the Russian Science Foundation (grant no. 22-23-00468). The research was carried out using the equipment of the shared research facilities of HPC computing resources at Lomonosov Moscow State University. The authors acknowledge partial support from MSU Shared Research Equipment Center ‘Technologies for obtaining new nanostructured materials and their complex study’, National Project ‘Science’ and MSU Program of Development.

Online Supplementary Materials

Supplementary data associated with this article can be found in the online version at doi: 10.1016/j.mencom.2024.02.005.

References

1 G. Bernardo, T. Lopes, D. G. Lidzey and A. Mendes, *Adv. Energy Mater.*, 2021, **11**, 2100342.

2 R. Rathanasamy, S. Sahoo, J. H. Lee, A. K. Das, M. Somasundaram, S. K. Palaniappan and S. Sivaraj, *J. Electron. Mater.*, 2021, **50**, 1845.

3 Y. Wakayama, R. Hayakawa, K. Higashiguchi and K. Matsuda, *J. Mater. Chem. C*, 2020, **8**, 10956.

4 C. Sun, P. Yang, Z. Nan, C. Tian, Y. Cai, J. Chen, F. Qi, H. Tian, L. Xie, L. Meng and Z. Wei, *Adv. Mater.*, 2023, **35**, 2205603.

5 Z. Zhao, S. Das and M. Zharnikov, *ACS Appl. Nano Mater.*, 2023, **6**, 2151.

6 X. Wang, C. Shen, J. Li, M. Zhang and P. Song, *Nanoscale Adv.*, 2023, **5**, 3267.

7 A. A. Popov, I. E. Kareev, N. B. Shustova, S. F. Lebedkin, S. H. Strauss, O. V. Boltalina and L. Dunsch, *Chem. – Eur. J.*, 2008, **14**, 107.

8 N. B. Tamm, V. A. Brotsman and S. I. Troyanov, *Mendeleev Commun.*, 2023, **33**, 821.

9 M. P. Kosaya, A. V. Rybalchenko, N. S. Lukonina, O. N. Mazaleva, I. N. Ioffe, V. Yu. Markov, S. I. Troyanov, L. N. Sidorov, N. B. Tamm and A. A. Goryunkov, *Chem. - Asian J.*, 2018, **13**, 1920.

10 K. P. Castro, Y. Jin, J. J. Rack, S. H. Strauss, O. V. Boltalina and A. A. Popov, *J. Phys. Chem. Lett.*, 2013, **4**, 2500.

11 N. Lou, Y. Li and L. Gan, *Angew. Chem., Int. Ed.*, 2017, **56**, 2403.

12 N. S. Lukonina, O. O. Semivrazhskaya, M. G. Apenova, N. M. Belov, S. I. Troyanov and A. A. Goryunkov, *Asian J. Org. Chem.*, 2019, **8**, 1924.

13 A. V. Rybalchenko, M. G. Apenova, O. O. Semivrazhskaya, N. M. Belov, V. Y. Markov, S. I. Troyanov, I. N. Ioffe, N. S. Lukonina, L. N. Sidorov, T. V. Magdesieva and A. A. Goryunkov, *Electrochim. Acta*, 2016, **191**, 980.

14 S. V. Gracheva, T. S. Yankova, M. P. Kosaya, V. A. Brotsman, I. N. Ioffe, N. S. Lukonina and A. A. Goryunkov, *Phys. Chem. Chem. Phys.*, 2022, **24**, 26998.

15 C. Bingel, *Chem. Ber.*, 1993, **126**, 1957.

16 X. Camps and A. Hirsch, *J. Chem. Soc., Perkin Trans. 1*, 1997, 1595.

17 Y. N. Biglova and A. G. Mustafin, *RSC Adv.*, 2019, **9**, 22428.

18 J. C. Hummelen, B. W. Knight, F. LePeq and F. Wudl, *J. Org. Chem.*, 1995, **60**, 532.

19 Y. N. Biglova, *Beilstein J. Org. Chem.*, 2021, **17**, 630.

20 M. Ueda, N. Imai, S. Yoshida, H. Yasuda, T. Fukuyama and I. Ryu, *Eur. J. Org. Chem.*, 2017, 6483.

21 M. H. Hall, H. Lu and P. B. Shevlin, *J. Am. Chem. Soc.*, 2001, **123**, 1349.

22 N. S. Ovchinnikova, D. V. Ignateva, N. B. Tamm, S. M. Avdoshenko, A. A. Goryunkov, I. N. Ioffe, V. Yu. Markov, S. I. Troyanov, L. N. Sidorov, M. A. Yurovskaya and E. Kemnitz, *New J. Chem.*, 2008, **32**, 89.

23 N. S. Ovchinnikova, A. A. Goryunkov, P. A. Khavrel, N. M. Belov, M. G. Apenova, I. N. Ioffe, M. A. Yurovskaya, S. I. Troyanov, L. N. Sidorov and E. Kemnitz, *Dalton Trans.*, 2011, **40**, 959.

24 K. Liosi, A. Romero-Rivera, O. Semivrazhskaya, C. D. Caniglia, M. Garcia-Borràs, N. Trapp, S. Osuna and Y. Yamakoshi, *Org. Lett.*, 2019, **21**, 5162.

25 V. A. Brotsman, N. S. Lukonina, N. A. Malkin, A. V. Rybalchenko, N. M. Belov and A. A. Goryunkov, *Phys. Chem. Chem. Phys.*, 2022, **24**, 16816.

26 O. O. Semivrazhskaya, N. M. Belov, A. V. Rybalchenko, V. Yu. Markov, I. N. Ioffe, N. S. Lukonina, S. I. Troyanov, E. Kemnitz and A. A. Goryunkov, *Eur. J. Org. Chem.*, 2018, 750.

27 V. A. Brotsman, V. P. Bogdanov, A. V. Rybalchenko, E. P. Galanicheva, N. M. Belov, V. Yu. Markov, N. S. Lukonina, I. N. Ioffe, S. I. Troyanov, E. Kemnitz and A. A. Goryunkov, *Chem. – Asian J.*, 2016, **11**, 1945.

28 D. N. Laikov, *Chem. Phys. Lett.*, 1997, **281**, 151.

29 J. P. Perdew, K. Burke and M. Ernzerhof, *Phys. Rev. Lett.*, 1996, **77**, 3865.

30 O. O. Semivrazhskaya, A. V. Rybalchenko, M. P. Kosaya, N. S. Lukonina, O. N. Mazaleva, I. N. Ioffe, S. I. Troyanov, N. B. Tamm and A. A. Goryunkov, *Electrochim. Acta*, 2017, **255**, 472.

31 C. M. Cardona, W. Li, A. E. Kaifer, D. Stockdale and G. C. Bazan, *Adv. Mater.*, 2011, **23**, 2367.

32 C. Adamo and V. Barone, *J. Chem. Phys.*, 1999, **110**, 6158.

33 F. Weigend and R. Ahlrichs, *Phys. Chem. Chem. Phys.*, 2005, **7**, 3297.

34 A. A. Granovsky, *Firefly, Version 8.2.0*, 2016.

35 M. W. Schmidt, K. K. Baldridge, J. A. Boatz, S. T. Elbert, M. S. Gordon, J. H. Jensen, S. Koseki, N. Matsunaga, K. A. Nguyen, S. Su, T. L. Windus, M. Dupuis and J. A. Montgomery, *J. Comput. Chem.*, 1993, **14**, 1347.

Received: 29th November 2023; Com. 23/7322